

Do Secondary and Tertiary Ammonium Cations Act as Structure-Directing Agents in the Formation of Layered Uranyl Selenites?

Philip M. Almond and Thomas E. Albrecht-Schmitt*

Department of Chemistry, Auburn University, Auburn, Alabama 36849

Received March 21, 2003

Two new layered uranyl selenites, $[C_4H_{12}N_2]_{0.5}[UO_2(HSeO_3)(SeO_3)]$ (**1**) and $[C_6H_{14}N_2]_{0.5}[UO_2(HSeO_3)(SeO_3)] \cdot 0.5H_2O \cdot 0.5CH_3CO_2H$ (**2**), have been isolated from mild hydrothermal reactions. The preparation of **1** was achieved by reacting $UO_2(C_2H_3O_2)_2 \cdot 2H_2O$ with H_2SeO_4 in the presence of piperazine at 130 °C for 2 d. Crystals of **2** were synthesized by reacting $UO_2(C_2H_3O_2)_2 \cdot 2H_2O$, H_2SeO_4 , and 1,4-diazabicyclo[2.2.2]octane at 150 °C for 2 d. The structure of **1** consists of UO_2^{2+} cations that are bound by bridging $HSeO_3^-$ anions and chelating/bridging SeO_3^{2-} anions to yield UO_7 pentagonal bipyramids. The joining of the uranyl moieties by the hydrogen selenite and selenite anions creates two-dimensional ${}_{\infty}^2[UO_2(HSeO_3)(SeO_3)]^-$ layers that extend in the *bc*-plane. The stereochemically active lone pair of electrons on the $HSeO_3^-$ and SeO_3^{2-} anions align along the *a*-axis making each layer polar. The ${}_{\infty}^2[UO_2(HSeO_3)(SeO_3)]^-$ layers and piperazinium cations stack in a AA'BAA'B sequence where two layers stack on one another without intervening piperazinium cations. While each ${}_{\infty}^2[UO_2(HSeO_3)(SeO_3)]^-$ layer is polar, in the AA' stacking, the polarity of the second sheet is reversed with respect to the first, yielding an overall structure that is centrosymmetric. The structure of **2** is constructed from uranyl cations that are bound by three bridging SeO_3^{2-} and two bridging $HSeO_3^-$ anions to create UO_7 pentagonal bipyramids. The linking of the uranyl cations by the $HSeO_3^-$ and SeO_3^{2-} anions creates ${}_{\infty}^2[UO_2(HSeO_3)(SeO_3)]^-$ layers that extend in the *ac*-plane. In **1** and **2**, the organic ammonium cations form hydrogen bonds with the anionic uranyl selenite layers. Crystallographic data: **1**, monoclinic, space group $P2_1/c$, $a = 10.9378(5)$ Å, $b = 8.6903(4)$ Å, $c = 9.9913(5)$ Å, $\beta = 90.3040(8)^\circ$, $Z = 4$; **2**, orthorhombic, space group $Pnma$, $a = 13.0858(8)$ Å, $b = 17.555(1)$ Å, $c = 10.5984(7)$ Å, $Z = 8$.

Introduction

Oxoanions possessing a stereochemically active lone pair of electrons have a propensity for aligning in the solid state to yield polar structures.^{1–3} This attribute gives rise to a number of important physical properties including second-harmonic generation (SHG) and ferroelectric behavior.^{1–3} A large number of main group elements are capable of exhibiting the inert pair effect and can therefore be incor-

porated into oxoanions used in the construction of solids with noncentrosymmetric (NCS) extended structures. Pb(II), Se(IV), Te(IV), and I(V) are particularly promising in this regard because in addition to forming relatively stable oxo species, large polarizabilities are observed in their bonds leading to enhancement of SHG responses. On the basis of these attributes, considerable efforts have been devoted to preparing purely inorganic selenites, SeO_3^{2-} , tellurites, TeO_3^{2-} , and iodates, IO_3^- , particularly in combination with early transition metals that are susceptible to second-order Jahn–Teller distortions, and to determining the structure–property relationships in these compounds. Examples of this family include $AVSeO_5$ ($A = Rb, Cs$),⁴ $A(VO)_3(SeO_3)_2$ ($A = NH_4, K, Rb, Cs$),^{4,5} $A_2(MoO_3)_3SeO_3$ ($A = NH_4, Rb, Cs, Tl$),^{6–8} $REMoO_2(IO_3)_4(OH)$ ($RE = La, Nd, Sm, Eu$),⁹

* To whom correspondence should be addressed. E-mail: albreth@auburn.edu.

- (1) Halasyamani, P. S.; Poeppelmeier, K. R. *Chem. Mater.* **1998**, *10*, 2753.
- (2) Rosker, M. J.; Marcy, H. O. New nonlinear materials for high-power frequency conversion: from the near-ultraviolet to the long-wave infrared. In *Novel Optical Materials and Applications*; Khoo, I.-C., Simoni, F., Umeton, C., Eds.; John Wiley & Sons: New York, 1997; pp 175–204.
- (3) Stucky, G. D.; Marder, S. R.; Sohn, J. E. Linear and Nonlinear Polarizability: A Primer. In *Materials for Nonlinear Optics*; Marder, S. R., Sohn, J. E., Stucky, G. D., Eds.; ACS Symposium Series 455; American Chemical Society: Washington, DC, 1991; pp 2–30.

- (4) Kwon, Y.-U.; Lee, K.-S.; Kim, Y. H. *Inorg. Chem.* **1996**, *35*, 1161.
- (5) Vaughey, J. T.; Harrison, W. T. A.; Dussack, L. L.; Jacobson, A. J. *Inorg. Chem.* **1994**, *33*, 4370.

AMoO₃(IO₃) (A = Rb, Cs),¹⁰ A[(VO)₂(IO₃)₃O₂] (A = NH₄, Rb, Cs),¹¹ and Na₂TeW₂O₉.¹² The latter four compounds have been shown to have large SHG responses ranging from 350 to 500× that of α-quartz.^{9–12}

Quite recently several reports have appeared that demonstrate that inorganic cations can be replaced with organic structure-directing agents in the preparation of novel transition metal selenites. For instance, the aqueous reaction of guanidinium carbonate with ZnO and SeO₂ results in the crystallization of [CN₃H₆]₄[Zn₃(SeO₃)₅], which contains porous zinc selenite layers.¹³ An organic–inorganic hybrid zinc selenite, [C₂H₈N₂]_{0.5}ZnSeO₃, is also known.¹⁴ However, here the ethylenediamine is not protonated and instead directly coordinates the Zn(II) centers to aid in the formation of a layered structure. Open-framework iron fluoroselenites with the general formula [A][Fe₂F₃(SeO₃)₃] (A = [C₄H₁₂N₂]_{0.5} or [C₄H₁₄N₃]_{0.5}) have also been prepared and show magnetic spin frustration.¹⁴ Vanadium selenites with organic cations are proving to be particularly rich, and a variety of molecular and extended structures are now recognized that range from small polyoxometalates such as [(C₄H₉)₄N]₃[V₃SeO₁₁]·0.5H₂O¹⁵ to two-dimensional, vanadyl(IV) and vanadyl(V) selenites with organic structure-directing agents¹⁶ and to the layered bimetallic compound [Cu(Phen)₂]₂V₂Se₂O₁₁, where-[Cu(Phen)]²⁺ units are used to link vanadium selenite substructures together.¹⁷ All of these compounds are centrosymmetric.

We have been addressing the role that the stereochemically active lone pair of electrons in certain oxoanions plays in the formation of a variety of actinyl(V) and actinyl(VI) compounds and thus far have prepared more than 30 uranyl iodates,¹⁸ selenites,¹⁹ and tellurites.²⁰ It is interesting to note

that from this group only PbUO₂(SeO₃)₂,^{19a} NpO₂(IO₃)₂,²¹ AnO₂(IO₃)₂·H₂O (An = Np, Pu),^{18h,i} and Na₈[(UO₂)₆-(TeO₃)₁₀]^{20a} are NCS. This attribute can be ascribed to the approximately linear nature of the actinyl cation that allows it to be placed on inversion centers if AnO₆ and AnO₈ tetragonal or hexagonal bipyramids are formed; even in the case of the more common AnO₇ pentagonal bipyramid, two such units are often related to one another through an inversion center.^{20a} Therefore, NCS structures containing actinyl cations are atypical²² but even in the absence of polar anions are still known, as demonstrated by Cs₂(UO₂)-(PO₄)₄(H₂O)₂, which crystallizes in the polar space group *Cmc*2₁.²³

Despite the centrosymmetric nature of most actinyl compounds with oxoanions containing nonbonding electrons, these electrons can still play critical roles in determining the dimensionality of uranyl phases. For instance, while most uranyl compounds adopt layered structures,²² the majority of uranyl iodates form one-dimensional chains.¹⁸ This also true of many naturally occurring and synthetic uranyl selenite^{19,24} and tellurite^{20,25} phases such as Cu₄[(UO₂)(SeO₃)₂](OH)₆^{24a} and Pb₂Cu₅[(UO₂)(SeO₃)₃]₂(OH)₆(H₂O)₂,^{24b} where one-dimensional uranyl selenite chains are observed. It is also important to recognize that the lone pair sometimes plays no apparent role at all, as is the case in some uranyl phases that contain Tl(I)^{18a,c} or Pb(II).^{18a,18c,26} In these compounds, the main group cations are acting as pseudo-alkali and alkaline-earth metals and in some instances form isostructural series with cations that have the same charge and approximate ionic radius.^{18a,c} This implies that the lone pair is

(6) Harrison, W. T. A.; Dussack, L. L.; Jacobson, A. J. *J. Solid State Chem.* **1996**, *125*, 234.
 (7) Harrison, W. T. A.; Dussack, L. L.; Jacobson, A. J. *Inorg. Chem.* **1994**, *33*, 6043.
 (8) Dussack, L. L.; Harrison, W. T. A.; Jacobson, A. J. *Mater. Res. Bull.* **1996**, *31*, 249.
 (9) Shehee, T. C.; Sykora, R. E.; Ok, K. M.; Halasyamani, P. S.; Albrecht-Schmitt, T. E. *Inorg. Chem.* **2003**, *42*, 457.
 (10) Sykora, R. E.; Ok, K. M.; Halasyamani, P. S.; Albrecht-Schmitt, T. E. *J. Am. Chem. Soc.* **2002**, *124*, 1951.
 (11) Sykora, R. E.; Ok, K. M.; Halasyamani, P. S.; Wells, D. M.; Albrecht-Schmitt, T. E. *Chem. Mater.* **2002**, *14*, 2741.
 (12) Goodey, J.; Broussard, J.; Halasyamani, P. S. *Chem. Mater.* **2002**, *14*, 3174.
 (13) Harrison, W. T. A.; Phillips, M. L. F.; Stanchfield, J.; Nenoff, T. M. *Angew. Chem., Int. Ed.* **2000**, *39*, 3808.
 (14) Choudhury, A.; Udaya Kumar, D.; Rao, C. N. R. *Angew. Chem., Int. Ed.* **2002**, *41*, 158.
 (15) Natano, H.; Ozeki, T.; Yagasaki, A. *Inorg. Chem.* **2001**, *40*, 1816.
 (16) Pasha, I.; Choudhury, A.; Rao, C. N. R. *Inorg. Chem.* **2003**, *42*, 409.
 (17) Shi, Z.; Zhang, D.; Feng, S.; Li, G.; Dai, Z.; Fu, W.; Chen, X.; Hua, J. *J. Chem. Soc., Dalton Trans.* **2002**, *9*, 1873.
 (18) (a) Bean, A. C.; Albrecht-Schmitt, T. E. *J. Solid State Chem.* **2001**, *161*, 416. (b) Bean, A. C.; Campana, C. F.; Kwon, O.; Albrecht-Schmitt, T. E. *J. Am. Chem. Soc.* **2001**, *123*, 8806. (c) Bean, A. C.; Ruf, M.; Albrecht-Schmitt, T. E. *Inorg. Chem.* **2001**, *40*, 3959. (d) Bean, A. C.; Peper, S. M.; Albrecht-Schmitt, T. E. *Chem. Mater.* **2001**, *13*, 1266. (e) Sykora, R. E.; Wells, D. M.; Albrecht-Schmitt, T. E. *Inorg. Chem.* **2002**, *41*, 2304. (f) Sykora, R. E.; McDaniel, S. M.; Wells, D. M.; Albrecht-Schmitt, T. E. *Inorg. Chem.* **2002**, *41*, 5126. (g) Bean, A. C.; Xu, Y.; Danis, J. A.; Albrecht-Schmitt, T. E.; Runde, W. *Inorg. Chem.* **2002**, *41*, 6775. (h) Runde, W.; Bean, A. C.; Albrecht-Schmitt, T. E.; Scott, B. L. *Chem. Commun.* **2003**, *4*, 478. (i) Bean, A. C.; Albrecht-Schmitt, T. E.; Scott, B. L.; Runde, W. *Inorg. Chem.* **2003**, in press.

(19) (a) Almond, P. M.; Albrecht-Schmitt, T. E. *Inorg. Chem.* **2002**, *41*, 5495. (b) Almond, P. M.; Peper, S. M.; Bakker, E.; Albrecht-Schmitt, T. E. *J. Solid State Chem.* **2002**, *168*, 358.
 (20) (a) Almond, P. M.; McKee, M. L.; Albrecht-Schmitt, T. E. *Angew. Chem., Int. Ed.* **2002**, *114*, 3576. (b) Almond, P. M.; Albrecht-Schmitt, T. E. *Inorg. Chem.* **2002**, *41*, 5495.
 (21) Albrecht-Schmitt, T. E.; Almond, P. M.; Sykora, R. E. *Inorg. Chem.* **2003**, *42*, 3788.
 (22) (a) Burns, P. C.; Ewing, R. C.; Hawthorne, F. C. *Can. Mineral.* **1997**, *35*, 1551. (b) Burns, P. C. In *Uranium: Mineralogy, Geochemistry and the Environment*; Burns, P. C., Finch, R., Eds.; Mineralogical Society of America: Washington, DC, 1999; Chapter 1. (c) Burns, P. C.; Miller, M. L.; Ewing, R. C. *Can. Mineral.* **1996**, *34*, 845.
 (23) Locock, A. J.; Burns, P. C. *J. Solid State Chem.* **2002**, *167*, 226.
 (24) (a) Ginderow, D.; Cesbron, F. *Acta Crystallogr.* **1983**, *C39*, 1605. (b) Ginderow, D.; Cesbron, F. *Acta Crystallogr.* **1983**, *C39*, 824. (c) Cooper, M. A.; Hawthorne, F. C. *Can. Mineral.* **1995**, *33*, 1103. (d) Cooper, M. A.; Hawthorne, F. C. *Can. Mineral.* **2001**, *39*, 797. (e) Vochten, R.; Blaton, N.; Peeters, O.; Deliens, M. *Can. Mineral.* **1996**, *34*, 1317. (f) Loopstra, B. O.; Brandenburg, N. P. *Acta Crystallogr.* **1978**, *B34*, 1335. (g) Mistryukov, V. E.; Michailov, Y. N. *Koord. Khim.* **1983**, *9*, 97. (h) Koshenlinna, M.; Mutikainen, I.; Leskelä, T.; Leskela, M. *Acta Chem. Scand.* **1997**, *51*, 264. (i) Koshenlinna, M.; Valkonen, J. *Acta Crystallogr.* **1996**, *C52*, 1857.
 (25) (a) Branstätter, F. *Tschermaks Mineral. Petrogr. Mitt.* **1981**, *29*, 1. (b) Swihart, G. H.; Gupta, P. K. S.; Schlemper, E. O.; Back, M. E. Gaines, R. V. *Am. Mineral.* **1993**, *78*, 835. (c) Meunier, G.; Galy, J. *Acta Crystallogr.* **1973**, *B29*, 1251. (d) Branstätter, F. *Z. Kristallogr.* **1981**, *155*, 193.
 (26) (a) Taylor, J. C.; Stuart, W. L.; Mumme, I. A. *J. Inorg. Nucl. Chem.* **1981**, *43*, 2419. (b) Piret, P.; Deliens, M.; Piret-Meunier, J.; Germain, G. *Bull. Mineral.* **1983**, *106*, 299. (c) Piret, P. *Bull. Mineral.* **1985**, *108*, 659. (d) Burns, P. C. *Am. Mineral.* **1997**, *82*, 1176. (e) Burns, P. C.; Hanchar, J. M. *Can. Mineral.* **1998**, *36*, 187. (f) Burns, P. C. *Am. Mineral.* **1999**, *84*, 1661. (g) Burns, P. C.; Hanchar, J. M. *Can. Mineral.* **1999**, *37*, 1483. (h) Li, Y.; Burns, P. C. *Can. Mineral.* **2000**, *38*, 1433.

unimportant in these phases in regard to the adoption of one structure type over another.

In an effort to further understand what role the stereochemically active lone pair of electrons on selenite anions plays in the formation of uranyl selenite compounds, we have expanded our efforts to include the use of aliphatic ammonium salts as counterions and have successfully prepared the first uranyl selenites that incorporate such organic structure-directing agents. These cations offer the advantage of increased size and structural versatility over alkali, alkaline-earth, and main group cations and are also capable of forming hydrogen bonds that may influence structure formation. Herein we report the hydrothermal syntheses and structures of the two-dimensional uranyl selenites $[\text{C}_4\text{H}_{12}\text{N}_2]_{0.5}[\text{UO}_2(\text{HSeO}_3)(\text{SeO}_3)]$ (**1**) and $[\text{C}_6\text{H}_{14}\text{N}_2]_{0.5}[\text{UO}_2(\text{HSeO}_3)(\text{SeO}_3)] \cdot 0.5\text{H}_2\text{O} \cdot 0.5\text{CH}_3\text{CO}_2\text{H}$ (**2**).

Experimental Section

Syntheses. $\text{UO}_2(\text{C}_2\text{H}_3\text{O}_2)_2 \cdot 2\text{H}_2\text{O}$ (98.0%, Alfa-Aesar), H_2SeO_4 (40% aqueous solution, Alfa-Aesar), piperazine (99%, Aldrich), and 1,4-diazabicyclo[2.2.2]octane (DABCO) (98%, Aldrich) were used as received. Distilled and Millipore-filtered water was used in all reactions. The resistance of the water was 18.2 M Ω . The PTFE liners used in these reactions were heated with distilled and Millipore-filtered water at 200 °C for 3 d prior to use. While the $\text{UO}_2(\text{C}_2\text{H}_3\text{O}_2)_2 \cdot 2\text{H}_2\text{O}$ contains depleted U, standard precautions for handling radioactive materials should be followed. Old sources of depleted U should not be used, as the daughter elements of natural decay are highly radioactive and present serious health risks.²⁷ SEM/EDX analyses were performed using a JEOL 840/Link Isis instrument. IR spectra were collected on a Nicolet 5PC FT-IR spectrometer from KBr pellets.

$[\text{C}_4\text{H}_{12}\text{N}_2]_{0.5}[\text{UO}_2(\text{HSeO}_3)(\text{SeO}_3)]$ (**1**). $\text{UO}_2(\text{C}_2\text{H}_3\text{O}_2)_2 \cdot 2\text{H}_2\text{O}$ (178 mg, 0.419 mmol), H_2SeO_4 (1 mL, 9.73 mmol), and piperazine (100 mg, 1.13 mmol) were loaded in a 23-mL PTFE-lined autoclave followed by the addition of 3 mL of water. The autoclave was sealed and placed in a preheated furnace for 2 d at 130 °C. The furnace was cooled at 9 °C/h to 23 °C. The solid product consisted of yellow tablets of **1**. The mother liquor was decanted from the crystals, and they were subsequently washed with methanol and allowed to dry. Yield: 190 mg (80% yield based on U). EDX analysis for **1** provided a U:Se ratio of 1:2. Anal. Calcd for $\text{C}_2\text{H}_8\text{N}_2\text{O}_8\text{Se}_2\text{U}$: C, 4.23; H, 1.14; N, 2.46. Found: C, 4.31; H, 1.22; N, 2.45. IR (KBr, cm^{-1}): 909 ($\nu_{3[\text{uranyl}]}$, s), 860 ($\nu_{1[\text{uranyl}]}$, m), 814 (ν_{SeO} , m, sh), 800 (ν_{SeO} , m), 734 (ν_{SeO} , s), 581 (δ_{SeO} , m), 476 (δ_{SeO} , s).

$[\text{C}_6\text{H}_{14}\text{N}_2]_{0.5}[\text{UO}_2(\text{HSeO}_3)(\text{SeO}_3)] \cdot 0.5\text{H}_2\text{O} \cdot 0.5\text{CH}_3\text{CO}_2\text{H}$ (**2**). $\text{UO}_2(\text{C}_2\text{H}_3\text{O}_2)_2 \cdot 2\text{H}_2\text{O}$ (178 mg, 0.419 mmol), H_2SeO_4 (1 mL, 9.73 mmol), and 1,4-diazabicyclo[2.2.2]octane (100 mg, 0.875 mmol) were loaded in a 23-mL PTFE lined autoclave. A 3 mL volume of water was then added. The autoclave was sealed and placed in a preheated furnace for 2 d at 150 °C. The furnace was cooled at 9 °C/h to 23 °C. The solid product consisted of yellow prisms of **2**. The mother liquor was decanted from the crystals, and they were subsequently washed with methanol and allowed to dry. Yield: 150 mg (58% yield based on U). EDX analysis for **2** provided a U:Se ratio of 1:2. Anal. Calcd for $\text{C}_4\text{H}_{11}\text{NO}_{9.5}\text{Se}_2\text{U}$: C, 7.73; H, 1.79; N, 2.26. Found: C, 6.97; H, 1.69; N, 2.55. Acceptable CHN

(27) In our laboratory, uranium starting materials are stored in a glovebox or vented drawer until needed. All manipulations are carried out while we are wearing gloves and eye protection. All products are stored in a fume hood solely designated for radioactive materials.

Table 1. Crystallographic Data for $[\text{C}_4\text{H}_{12}\text{N}_2]_{0.5}[\text{UO}_2(\text{HSeO}_3)(\text{SeO}_3)]$ (**1**) and $[\text{C}_6\text{H}_{14}\text{N}_2]_{0.5}[\text{UO}_2(\text{HSeO}_3)(\text{SeO}_3)] \cdot 0.5\text{H}_2\text{O} \cdot 0.5\text{CH}_3\text{CO}_2\text{H}$ (**2**)

param	1	2
color and habit	yellow tablet	yellow prism
formula mass (amu)	568.03	621.09
space group	$P2_1/c$ (No. 14)	$Pnma$ (No. 62)
a (Å)	10.9378(5)	13.0858(8)
b (Å)	8.6903(4)	17.555(1)
c (Å)	9.9913(5)	10.5984(7)
α (deg)	90	90
β (deg)	90.3040(8)	90
γ (deg)	90	90
V (Å ³)	949.69(8)	2434.7(3)
Z	4	8
T (°C)	−80	−80
λ (Å)	0.710 73	0.710 73
ρ_{calcd} (g cm^{-3})	3.973	3.389
μ (Mo $K\alpha$) (cm^{-1})	247.77	193.54
$R(F)$ for $F_o^2 > 2\sigma(F_o^2)^a$	0.0194	0.0297
$R_w(F_o^2)^b$	0.0515	0.0619

$$^a R(F) = \sum ||F_o| - |F_c|| / \sum |F_o|. \quad ^b R_w(F_o^2) = [\sum (w(F_o^2 - F_c^2)^2) / \sum w F_o^4]^{1/2}.$$

analyses were not obtained because of a small amount of elemental Se coating on bulk samples of crystals. IR (KBr, cm^{-1}): 904 ($\nu_{3[\text{uranyl}]}$, s), 876 ($\nu_{1[\text{uranyl}]}$, m), 778 (ν_{SeO} , m), 712 (ν_{SeO} , s), 655 (ν_{SeO} , w, br), 490 (δ_{SeO} , m), 454 (δ_{SeO} , m).

Crystallographic Studies. Crystals of $[\text{C}_4\text{H}_{12}\text{N}_2]_{0.5}[\text{UO}_2(\text{HSeO}_3)(\text{SeO}_3)]$ (**1**) and $[\text{C}_6\text{H}_{14}\text{N}_2]_{0.5}[\text{UO}_2(\text{HSeO}_3)(\text{SeO}_3)] \cdot 0.5\text{H}_2\text{O} \cdot 0.5\text{CH}_3\text{CO}_2\text{H}$ (**2**) were mounted on glass fibers and aligned on a Bruker SMART APEX CCD X-ray diffractometer. Intensity measurements were performed using graphite-monochromated Mo $K\alpha$ radiation from a sealed tube and a monochromator. SMART was used for preliminary determination of the cell constants and data collection control. For all compounds, the intensities of reflections of a sphere were collected by a combination of 3 sets of exposures (frames). Each set had a different ϕ angle for the crystal, and each exposure covered a range of 0.3° in ω . A total of 1800 frames were collected with an exposure time per frame of 60 s for **1** and 30 s for **2**.

For **1** and **2**, determination of integral intensities and global cell refinement were performed with the Bruker SAINT (v 6.02) software package using a narrow-frame integration algorithm. A faced-indexed analytical absorption correction was initially applied using XPREP.²⁸ Individual shells of unmerged data were corrected analytically and exported in the same format. These files were subsequently treated with a semiempirical absorption correction by SADABS²⁹ with a μt parameter of 0.³⁰ The program suite SHELXTL (v 5.1) was used for space group determination (XPREP), direct methods structure solution (XS), and least-squares refinement (XL).²⁸ The final refinements included anisotropic displacement parameters for all non-hydrogen atoms and a secondary extinction parameter. Some crystallographic details are listed in Table 1. Additional details can be found in the Supporting Information.

Results and Discussion

Syntheses. As noted by Rao and co-workers,¹⁶ the primary challenge in preparing selenites with structure-directing amines is that the latter are reducing and the selenate/selenite

(28) Sheldrick, G. M. *SHELXTL PC, Version 5.0, An Integrated System for Solving, Refining, and Displaying Crystal Structures from Diffraction Data*; Siemens Analytical X-ray Instruments, Inc.: Madison, WI, 1994.

(29) SADABS. Program for absorption correction using SMART CCD based on the method of Blessing: Blessing, R. H. *Acta Crystallogr.* **1995**, *A51*, 33.

(30) Huang, F. Q.; Ibers, J. A. *Inorg. Chem.* **2001**, *40*, 2602.

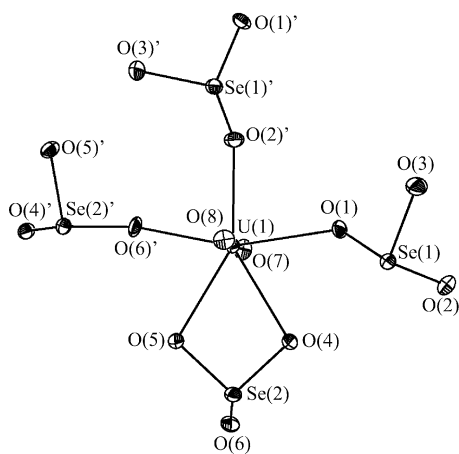


Figure 1. UO_7 pentagonal bipyramid in $[\text{C}_4\text{H}_{12}\text{N}_2]_{0.5}[\text{UO}_2(\text{HSeO}_3)(\text{SeO}_3)]$ (**1**) formed from the ligation of a UO_2^{2+} cations by bridging HSeO_3^- and chelating/bridging SeO_3^{2-} anions. The 50% probability ellipsoids are depicted.

anions can act as oxidizing agents. Therefore, substantial amine oxidation and decomposition is expected to occur under hydrothermal conditions. The syntheses of the present uranyl selenites containing structure-directing amines, $[\text{C}_4\text{H}_{12}\text{N}_2]_{0.5}[\text{UO}_2(\text{HSeO}_3)(\text{SeO}_3)]$ (**1**) and $[\text{C}_6\text{H}_{14}\text{N}_2]_{0.5}[\text{UO}_2(\text{HSeO}_3)(\text{SeO}_3)] \cdot 0.5\text{H}_2\text{O} \cdot 0.5\text{CH}_3\text{CO}_2\text{H}$ (**2**), were achieved by running the appropriate reactions at relatively low temperatures for reduced durations compared to what we typically employ. The synthesis of **1** was accomplished by reacting $\text{UO}_2(\text{C}_2\text{H}_3\text{O}_2)_2 \cdot 2\text{H}_2\text{O}$ with H_2SeO_4 in the presence of piperazine at 130°C for 2 d, and **2** was prepared by substituting piperazine with 1,4-diazabicyclo[2.2.2]octane (DABCO) and increasing the temperature to 150°C .

There are only small changes in pH that occur during the preparation of **1** and **2**. The initial pH of the reaction mixture that leads to the formation of **1** is 1.18, while the pH of the final mother liquor is 1.27. Likewise, the pH of the reaction that yields **2** only changes from an initial pH of 1.13 to a final pH of 1.29. Both preparations were temperature sensitive, and **1** was not isolated from reactions that were run above 130°C , whereas crystals of **2** can still be grown from reactions with temperatures up to 150°C . Presumably the increased stability of DABCO with respect to piperazine under oxidizing conditions accounts for this observation.¹⁶ Furthermore, unlike the preparation of purely inorganic uranyl selenites, which calls for the use of SeO_2 ,¹⁹ both **1** and **2** only formed when selenic acid was used as a source of selenite. Similar observations were made in the preparation of uranyl,^{18b,i} molybdenyl,¹⁰ and vanadyl iodates,¹¹ where metaperiodate, IO_4^- , had to be used as a precursor to IO_3^- . The vanadyl selenite, $[\text{DABCOH}_2]_{0.5}[(\text{VO})(\text{HSeO}_3)(\text{SeO}_3)] \cdot \text{H}_2\text{O}$, was also prepared by using H_2SeO_4 as the source of SeO_3^{2-} .¹⁶

Structures. $[\text{C}_4\text{H}_{12}\text{N}_2]_{0.5}[\text{UO}_2(\text{HSeO}_3)(\text{SeO}_3)]$ (**1**). The uranyl, UO_2^{2+} , cations in **1** are bound by bridging HSeO_3^- anions and chelating/bridging SeO_3^{2-} anions to yield a UO_7 pentagonal bipyramid as shown in Figure 1. As expected, the uranyl cations are approximately linear with an $\text{O}=\text{U}=\text{O}$ angle of $177.5(1)^\circ$, and there are two short $\text{U}=\text{O}$ distances of $1.783(3)$ and $1.784(3)$ Å (Table 2). The remaining five

Table 2. Selected Bond Distances (Å) for $[\text{C}_4\text{H}_{12}\text{N}_2]_{0.5}[\text{UO}_2(\text{HSeO}_3)(\text{SeO}_3)]$ (**1**)

$\text{U}(1)-\text{O}(1)$	2.385(3)	$\text{Se}(1)-\text{O}(1)$	1.697(3)
$\text{U}(1)-\text{O}(2)$	2.358(3)	$\text{Se}(1)-\text{O}(2)$	1.680(3)
$\text{U}(1)-\text{O}(4)$	2.458(3)	$\text{Se}(1)-\text{O}(3)$	1.749(3) (OH)
$\text{U}(1)-\text{O}(5)$	2.440(3)	$\text{Se}(2)-\text{O}(4)$	1.704(3)
$\text{U}(1)-\text{O}(6)$	2.299(3)	$\text{Se}(2)-\text{O}(5)$	1.708(3)
$\text{U}(1)-\text{O}(7)$ (U=O)	1.783(3)	$\text{Se}(2)-\text{O}(6)$	1.680(3)
$\text{U}(1)-\text{O}(8)$ (U=O)	1.784(3)		

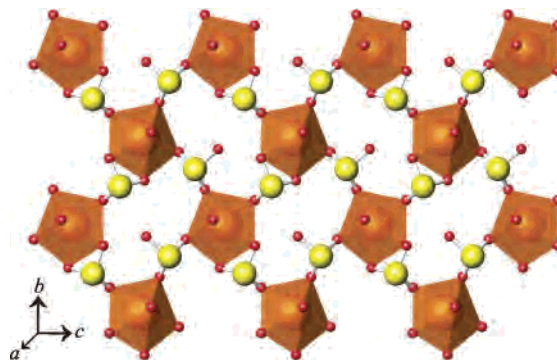


Figure 2. View down the a -axis showing the two-dimensional $[\text{UO}_2(\text{HSeO}_3)(\text{SeO}_3)]^-$ layers that extend in the bc -plane in $[\text{C}_4\text{H}_{12}\text{N}_2]_{0.5}[\text{UO}_2(\text{HSeO}_3)(\text{SeO}_3)]$ (**1**). The stereochemically active lone pair of electrons on both the HSeO_3^- and SeO_3^{2-} anions are aligned along the a -axis.

$\text{U}-\text{O}$ distances in the equatorial plane range from $2.299(3)$ to $2.458(3)$ Å and are within normal limits. The bond valence sum for the U atom in **1** is 5.90, which is consistent with U(VI).^{22a} The assignments of the HSeO_3^- and SeO_3^{2-} anions in **1** are based on several factors. First, the selenite anions containing Se(2) utilize all three oxygen atoms to coordinate U(VI) centers. Second, the $\text{Se}-\text{O}$ bonds around Se(2) are reasonably uniform and vary only from $1.680(3)$ to $1.708(3)$ Å. In contrast, the $[\text{SeO}_3]$ unit containing Se(1) only uses two of its oxo atoms to bind uranium, and the remain oxo atom is terminal. The $\text{Se}-\text{O}$ bond distance to the nominally terminal oxygen atom is $1.749(3)$ Å, which is substantially longer than the other two $\text{Se}-\text{O}$ bonds of $1.697(3)$ and $1.680(3)$ Å. Finally, the bond valence sum of this oxygen atom is 1.20.^{31,32} All of these factors, as well as charge neutrality requirements, support this being an HSeO_3^- anion.

The joining of the uranyl moieties by the hydrogen selenite and selenite anions creates two-dimensional $[\text{UO}_2(\text{HSeO}_3)(\text{SeO}_3)]^-$ layers that extend in the bc -plane. Part of one of these layers is illustrated in Figure 2. As can be seen in this figure, fused rings are found within the sheets that are created from four uranium centers, two HSeO_3^- anions, and two SeO_3^{2-} anions. The selenite anions share a common uranium atom, as do the two hydrogen selenite anions. When compared with other known uranyl selenites with layered uranium oxide topologies, it becomes apparent that the sheets found in **1** bear some similarities with $\text{Pb}[\text{UO}_2(\text{SeO}_3)_2]$,^{19a} but are quite distinct from $\text{A}[(\text{UO}_2)(\text{HSeO}_3)(\text{SeO}_3)]$ ($\text{A} = \text{NH}_4, \text{K}, \text{Rb}, \text{Cs}, \text{Tl}$),^{19,24i} $\text{Ba}[\text{UO}_2(\text{SeO}_3)_2]$,^{19b} and the minerals guilleminite, $\text{Ba}[(\text{UO}_2)_3(\text{SeO}_3)_2\text{O}_2](\text{H}_2\text{O})_3$,^{24c} and marthozite, $\text{Cu}[(\text{UO}_2)_3(\text{SeO}_3)_2\text{O}_2](\text{H}_2\text{O})_8$,^{24d} that also adopt layered structures. $\text{Ba}[\text{UO}_2(\text{SeO}_3)_2]$ also contains layers formed from fused

(31) Brown, I. D.; Altermatt, D. *Acta Crystallogr.* **1985**, *B41*, 244.

(32) Bressé, N. E.; O'Keeffe, M. *Acta Crystallogr.* **1991**, *B47*, 192.

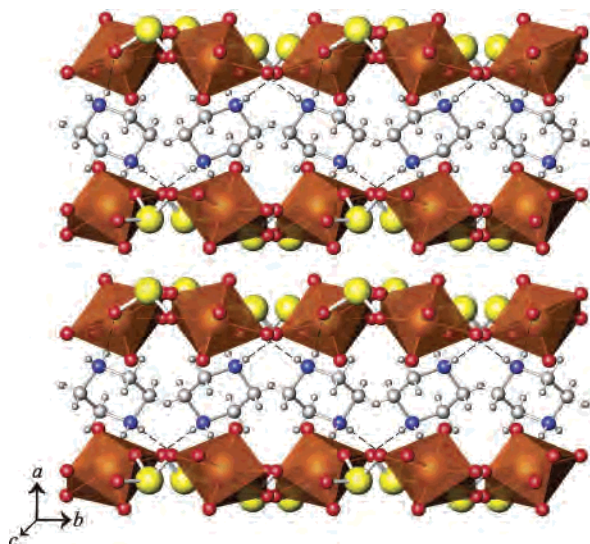


Figure 3. $\infty[\text{UO}_2(\text{HSeO}_3)(\text{SeO}_3)]^-$ layers and piperazinium cations in $[\text{C}_6\text{H}_{14}\text{N}_2]_{0.5}[\text{UO}_2(\text{HSeO}_3)(\text{SeO}_3)]$ (**1**) stack in an AA'BAA'B sequence where two $\infty[\text{UO}_2(\text{HSeO}_3)(\text{SeO}_3)]^-$ layers stack on one another without intervening piperazinium cations. While each $\infty[\text{UO}_2(\text{HSeO}_3)(\text{SeO}_3)]^-$ layer is polar, in the AA' stacking, the polarity of the second sheet is reversed with respect to the first, yielding an overall structure that is centrosymmetric. The piperazinium cations form hydrogen-bonding interactions with the hydrogen selenite anions to stitch the structure together.

uranyl selenite rings. However, these rings contain six uranyl cations and six SeO_3^{2-} anions. $\text{Pb}[\text{UO}_2(\text{SeO}_3)_2]$, on the other hand, does contain four uranyl moieties and four selenite anions in a ring, as found in **1**. However, the chelating/bridging and solely bridging selenite anions in $\text{Pb}[\text{UO}_2(\text{SeO}_3)_2]$ alternate within the ring, which does not occur in **1**. We have also compared the sheets in **1** with other known uranyl phases with sheet topologies based on pentagons and triangles and have not found an identical structure.^{22c,33} We therefore conclude that **1** has a new anionic uranyl sheet topology.

The stacking arrangement of the $\infty[\text{UO}_2(\text{HSeO}_3)(\text{SeO}_3)]^-$ layers and piperazinium cations in **1** is quite unusual for a layered uranyl structure in that alternating cations and uranyl-containing layers are not found. Rather two layers stack on one another without intervening piperazinium cations to yield an AA'BAA'B sequence as shown in Figure 3. The distance between uranium planes separated by piperazinium cations is 6.256(3) Å, while the direct stacking distance is 4.682(3) Å. The piperazinium cations form hydrogen-bonding interactions of 2.83(5) and 2.82(5) Å between N(1) and O(3) of

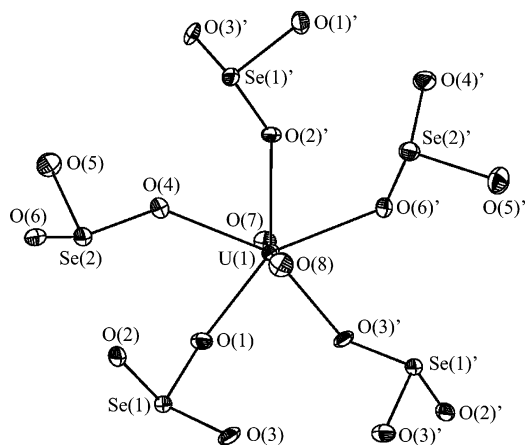


Figure 4. UO_7 pentagonal bipyramidal structural building units in $[\text{C}_6\text{H}_{14}\text{N}_2]_{0.5}[\text{UO}_2(\text{HSeO}_3)(\text{SeO}_3)] \cdot 0.5\text{H}_2\text{O} \cdot 0.5\text{CH}_3\text{CO}_2\text{H}$ (**2**) that are formed from uranyl cations that are bound by three bridging SeO_3^{2-} anions and two bridging HSeO_3^- anions. The 50% probability ellipsoids are depicted.

Table 3. Selected Bond Distances (Å) for $[\text{C}_6\text{H}_{14}\text{N}_2]_{0.5}[\text{UO}_2(\text{HSeO}_3)(\text{SeO}_3)] \cdot 0.5\text{H}_2\text{O} \cdot 0.5\text{CH}_3\text{CO}_2\text{H}$ (**2**)

U(1)–O(1)	2.312(4)	Se(1)–O(1)	1.700(4)
U(1)–O(2)	2.369(4)	Se(1)–O(2)	1.681(4)
U(1)–O(3)	2.348(4)	Se(1)–O(3)	1.700(4)
U(1)–O(4)	2.404(4)	Se(2)–O(4)	1.655(4)
U(1)–O(6)	2.451(4)	Se(2)–O(5)	1.771(4) (OH)
U(1)–O(7) (U=O)	1.786(4)	Se(2)–O(6)	1.699(4)
U(1)–O(8) (U=O)	1.788(4)		

the hydrogen selenite and O(4) of the selenite anions to stitch the structure together. An examination of an individual $\infty[\text{UO}_2(\text{HSeO}_3)(\text{SeO}_3)]^-$ layer shows that the selenite and hydrogen selenite anions are aligned with their stereochemically active lone pair of electrons pointed toward one side of the sheet, making each sheet polar. However, in the AA' stacking, the polarity of the second sheet is reversed with respect to the first, yielding an overall structure that is centrosymmetric.

$[\text{C}_6\text{H}_{14}\text{N}_2]_{0.5}[\text{UO}_2(\text{HSeO}_3)(\text{SeO}_3)] \cdot 0.5\text{H}_2\text{O} \cdot 0.5\text{CH}_3\text{CO}_2\text{H}$ (**2**). The structure of **2** is constructed from uranyl, UO_2^{2+} , cations that are bound by five bridging SeO_3^{2-} anions to create UO_7 pentagonal bipyramids as shown in Figure 4. The uranyl cations are approximately linear with $\text{O}=\text{U}=\text{O}$ angles of $177.7(2)^\circ$, and the uranyl oxo distances are 1.786(4) and 1.788(4) Å (Table 3). The U–O distances in the pentagonal plane are typical and range from 2.312(4) to 2.451(4) Å. The bond valence sum for the U atom in **2** is 5.94, which is consistent with U(VI).^{22a}

There are two types of bridging selenite anions in **2**, although neither is chelating as found in **1**. The selenite anion containing Se(1) uses all three of its oxygen atoms to bridge between three uranium centers. The second selenite anion containing Se(2) only uses two of its oxygen atoms to bind two uranyl cations. The remaining oxygen atom on Se(2) is terminal and with a Se–O bond distance of 1.771(4) Å is much longer than the average of the remaining Se–O distances of 1.677(4) Å. Furthermore, the bond valence sum of the terminal oxygen atom is 1.11, which when combined with the long Se–O bond distance leads us to conclude that that this oxygen atom is protonated.^{31,32} This distance is quite similar to the average Se–OH bond distances of 1.761(4) Å

(33) For some examples of newly recognized uranyl sheet topologies, see: (a) Krivovichev, S. V.; Burns, P. C. *Solid State Sci.* **2003**, *5*, 373. (b) Kim, J.-Y.; Norquist, A. J.; O'Hare, D. *Chem. Mater.* **2003**, *15*, 1970. (c) Burns, P. C.; Deely, K. M. *Can. Mineral.* **2002**, *40*, 1579. (d) Krivovichev, S. V.; Cahill, C. L.; Burns, P. C. *Inorg. Chem.* **2002**, *41*, 34. (e) Krivovichev, S. V.; Burns, P. C. *Inorg. Chem.* **2002**, *41*, 4108. (f) Norquist, A. J.; Thomas, P. M.; Doran, M. B.; O'Hare, D. *Chem. Mater.* **2002**, *14*, 5179. (g) Saadi, M.; Dion, C.; Abraham, F. *J. Solid State Chem.* **2000**, *150*, 72. (h) Burns, P. C.; Hill, F. C. *Can. Mineral.* **2000**, *38*, 163. (i) Cahill, C. L.; Burns, P. C. *Am. Mineral.* **2000**, *85*, 1294. (j) Krivovichev, S. V.; Burns, P. C. *Can. Mineral.* **2000**, *38*, 847. (k) Burns, P. C. *Am. Mineral.* **1999**, *84*, 1661. (l) Hill, F. C.; Burns, P. C. *Can. Mineral.* **1999**, *37*, 1283. (m) Burns, P. C.; Hanchar, J. M. *Can. Mineral.* **1999**, *37*, 1483. (n) Burns, P. C. *Can. Mineral.* **1998**, *36*, 187. (o) Guesdon, A.; Raveau, B. *Chem. Mater.* **1998**, *10*, 3471.

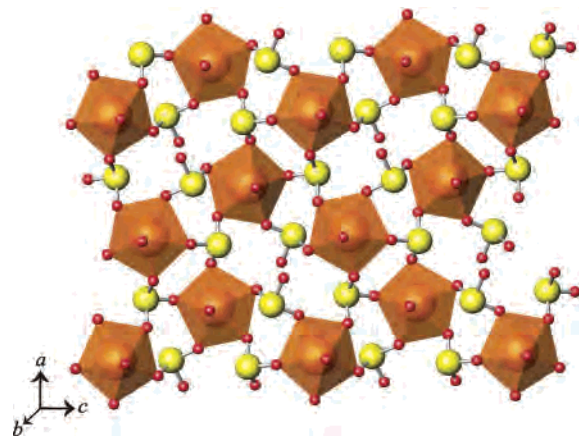


Figure 5. Illustration of part of a ${}^2_{\infty}[\text{UO}_2(\text{HSeO}_3)(\text{SeO}_3)]^-$ layer in $[\text{C}_6\text{H}_{14}\text{N}_2]_{0.5}[\text{UO}_2(\text{HSeO}_3)(\text{SeO}_3)] \cdot 0.5\text{H}_2\text{O} \cdot 0.5\text{CH}_3\text{CO}_2\text{H}$ (**2**) viewed down (010).

in $\text{A}[(\text{UO}_2)(\text{HSeO}_3)(\text{SeO}_3)]$ ($\text{A} = \text{NH}_4, \text{K}, \text{Rb}, \text{Cs}, \text{Tl}$),^{19,24i} which contains HSeO_3^- anions in the same bonding arrangement. This distance also compares well with the $\text{Se}-\text{OH}$ distance of 1.749(3) Å in **1**.

The linking of the uranyl cations by the HSeO_3^- and SeO_3^{2-} anions creates ${}^2_{\infty}[\text{UO}_2(\text{HSeO}_3)(\text{SeO}_3)]^-$ layers that extend in the ac -plane. Part of one of these layers is shown in Figure 5. Examination of the topology of these layers demonstrates that they are essentially the same as those in $\text{A}[(\text{UO}_2)(\text{HSeO}_3)(\text{SeO}_3)]$ ($\text{A} = \text{NH}_4, \text{K}, \text{Rb}, \text{Cs}, \text{Tl}$).^{19,24i} These layers can also be related to those found in a series of uranyl molybdates with sheets of the formula $[\text{UO}_2(\text{MoO}_4)_2]^{2-}$ by removing one of the vertexes from the MoO_4^{2-} tetrahedra.³⁴ $[\text{DABCOH}_2]_{0.5}[(\text{VO})(\text{HSeO}_3)(\text{SeO}_3)] \cdot \text{H}_2\text{O}$ ¹⁶ also has a sheet topology very similar to that of $\text{A}[(\text{UO}_2)(\text{HSeO}_3)(\text{SeO}_3)]$ ($\text{A} = \text{NH}_4, \text{K}, \text{Rb}, \text{Cs}, \text{Tl}$)^{19,24i} and $[\text{UO}_2(\text{MoO}_4)_2]^{2-}$ and can be related to these uranyl phases by removing a vertex from the UO_7 polyhedra.

The diprotonated $[\text{DABCOH}_2]^{2+}$ cations, acetic acid (derived from the uranyl acetate starting material), and water molecules separate the ${}^2_{\infty}[\text{UO}_2(\text{HSeO}_3)(\text{SeO}_3)]^-$ layers from one another creating a spacing of approximately 8.8 Å between uranium atom planes. In addition, the acetic acid forms a short $\text{O} \cdots \text{O}$ contact of 2.59(7) Å with the water molecule indicating a hydrogen bond. Other than this hydrogen bond, the next closest potential contacts are between the O(10) atom from the acetic acid and one of the ethylene moieties from the $[\text{DABCOH}_2]^{2+}$ cations. These interactions exceed 3.2 Å, and an extended hydrogen-bonding network is not formed parallel to the layers. However, the $[\text{DABCOH}_2]^{2+}$ cations are oriented with their ammonium moieties directed to uranyl selenites above and below the cations, as shown in Figure 6. Short $\text{N} \cdots \text{O}$ contacts of 2.82-(7) Å are observed between the N(1) atom and the O(3) atom of the selenite anions. Therefore, the hydrogen bonding between $[\text{DABCOH}_2]^{2+}$ cations and the ${}^2_{\infty}[\text{UO}_2(\text{HSeO}_3)(\text{SeO}_3)]^-$ layers imparts three-dimensional crystallinity to the structure.

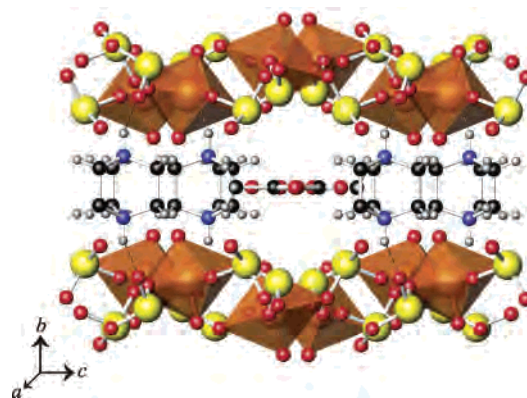


Figure 6. $[\text{C}_6\text{H}_{14}\text{N}_2]^{2+}$ cations in $[\text{C}_6\text{H}_{14}\text{N}_2]_{0.5}[\text{UO}_2(\text{HSeO}_3)(\text{SeO}_3)] \cdot 0.5\text{H}_2\text{O} \cdot 0.5\text{CH}_3\text{CO}_2\text{H}$ (**2**) form hydrogen bonds with the oxygen atoms from the selenite anions in the ${}^2_{\infty}[\text{UO}_2(\text{HSeO}_3)(\text{SeO}_3)]^-$ layers. The water and acetic acid molecules are interspersed with the $[\text{C}_6\text{H}_{14}\text{N}_2]^{2+}$ cations.

Conclusions

While the terms template and structure-directing are almost universally applied when organoammonium cations are used as counterions in the hydrothermal syntheses of inorganic framework compounds, it is often difficult to prove that these cations are doing anything more than balancing charge and filling space in most cases.³⁵ This is aptly illustrated by the structures of **1** and **2**. In **1** we find a new anionic sheet topology, which provides some indication that the piperazinium cations have a structure-directing effect that has not been observed thus far when inorganic cations have been employed. In contrast, the observation that the $[\text{DABCOH}_2]^{2+}$ cation yields the same topology as structurally unrelated alkali metal and Ti^+ cations indicates that the $[\text{DABCOH}_2]^{2+}$ cation is not acting as a template or structure-directing agent but rather is simply balancing charge and filling space between the layers. The fact that organoammonium cations can indeed yield new uranyl selenite structure types in some cases is quite promising. Furthermore, even though the overall structure of **1** is centrosymmetric, this compound does contain polar ${}^2_{\infty}[\text{UO}_2(\text{HSeO}_3)(\text{SeO}_3)]^-$ layers, which means that we are closer to achieving the preparation of a polar uranyl selenite containing an organic structure-directing agent.

Acknowledgment. This work was supported by the U.S. Department of Energy, Office of Basic Energy Sciences, Heavy Elements Program (Grant No. DE-FG02-01ER15187).

Supporting Information Available: X-ray crystallographic files for $[\text{C}_4\text{H}_{12}\text{N}_2]_{0.5}[\text{UO}_2(\text{HSeO}_3)(\text{SeO}_3)]$ (**1**) and $[\text{C}_6\text{H}_{14}\text{N}_2]_{0.5}[\text{UO}_2(\text{HSeO}_3)(\text{SeO}_3)] \cdot 0.5\text{H}_2\text{O} \cdot 0.5\text{CH}_3\text{CO}_2\text{H}$ (**2**) in CIF format. This material is available free of charge via the Internet at <http://pubs.acs.org>.

IC034308D

(34) Krivovichev, S. V.; Burns, P. C. *J. Solid State Chem.* **2003**, *170*, 106.

(35) Davis, M. E.; Lobo, R. F. *Chem. Mater.* **1992**, *4*, 756.